1 Higher Order Fields

1.1 Introduction

Beam-based high order field measurements have been carried out in the LHC since its first Run [1, 2], via chromaticity studies. Those measurements, made by varying the RF frequency while observing the resulting tune change, have been performed with a momentum offset of up to $\delta = \pm 2.2 \times 10^{-3}$, which led to the observation of the third order term of the non-linear chromaticity.

During the commissioning of Run 3 in 2022, a new collimator sequence has been introduced, allowing wider momentum offset measurements, within $\delta \in [-3.2 \times 10^{-3}, 3.7 \times 10^{-3}]$. This improved setup led to the observation of the fourth and fifth order terms at injection energy. Those terms, denoted $Q^{(4)}$ and $Q^{(5)}$ respectively in Eq. (1.1), are produced to first order by dodecapoles and decatetrapoles. Dodecapoles being powered off at injection and decatetrapoles being absent from the lattice, those fields originate from the field errors of the various magnets installed in the LHC.

$$Q(\delta) = Q_0 + Q'\delta + \frac{1}{2!}Q''\delta^2 + \frac{1}{3!}Q'''\delta^3 + \frac{1}{4!}Q^{(4)}\delta^4 + \frac{1}{5!}Q^{(5)}\delta^5 + O(\delta^6). \tag{1.1}$$

In addition to completing the measurements of high-order fields through chromaticity scans, turn-by-turn measurements were also conducted. High amplitude kicks indeed made it possible to observe dodecapolar RDTs in the LHC for the first time.

1.2 Chromaticity

1.2.1 Procedure

As described in **??**, the momentum offset δ is related to the RF frequency and the momentum compaction factor. This relation is given as a simplified form in Eq. (1.2). The model α_c for the LHC injection optics

is 3.48×10^{-4} for beam 1 and 3.47×10^{-4} for beam 2. Via this relation, a change of 140Hz of the RF frequency corresponds to a momentum offset of about -0.001.

$$\delta = -\frac{1}{\alpha_c} \cdot \frac{\Delta f_{RF}}{f_{RF,nominal}}. \tag{1.2}$$

To properly characterize higher orders of the chromaticity function and ensure quality measurements, several steps are required. The tune measured during chromaticity scans can exhibit jitter and resonance lines may appear, requiring thorough data cleaning to either reject problematic data points or reduce error bars. The simplified Eq. (1.2), describing δ, has been sufficient for reliably measuring up to the third order chromaticity. However, this relation also needs verification.

Noise and Spectral Lines

Noise lines, due to electronics, can be seen in the raw data obtained from the BBQ tune system. Occasionally, when those resonances are strong, their frequency peak can be mistaken as the tune and logged as such by the system. This yield large uncertainties in the measurement when data points can't properly be classified as outliers. A tune measurement presenting this issue is showed in Fig. 1.1.

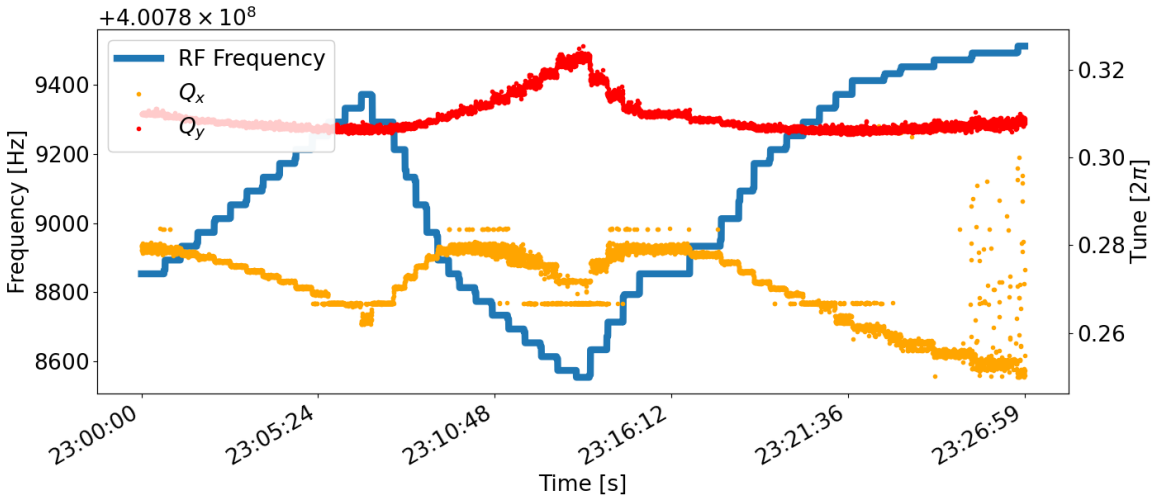

Figure 1.1: Shift of the tune by variation of the RF. Noise lines can appear in some cases, making the tune error bar large or downright unusable.

A solution to this issue is to use the raw data extracted from the BBQ system. From there, a spectrogram clearly shows the noise lines, as seen in Fig. 1.2. Those lines have been repeatedly identified over several measurements and confirmed to be fixed. The highest peak of the spectrogram

can thus be safely identified by removing those resonances, yielding a cleaner measurement. It is also to be added that the BBQ requires to set a tune window, which can be forgotten. By analyzing the raw data, it is ensured that the measurement has usable data and does not try to measure noise.

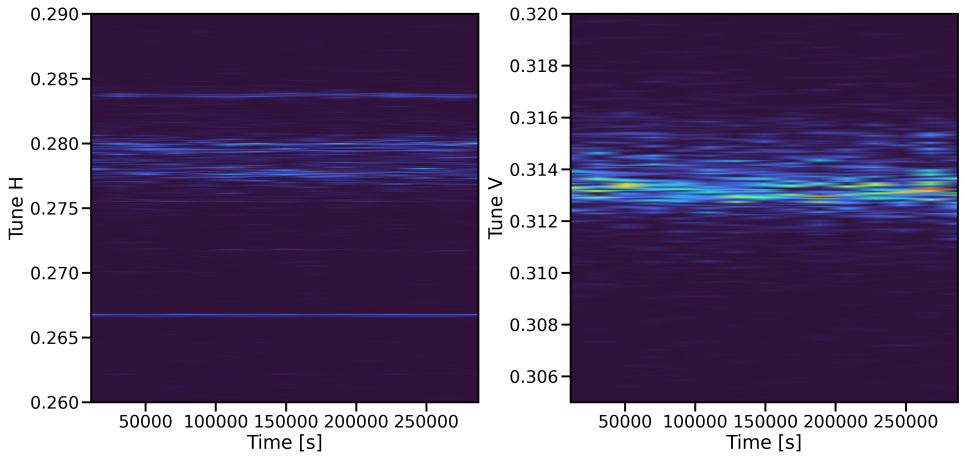

Figure 1.2: Tune spectrogram obtained via BBQ system. Strong resonance lines can be seen above and below where the tune really is, causing the wrong frequency peak to be identified as the tune.

Momentum Compaction Factor

Rather than a constant, the momentum compaction factor can be expressed as an expansion, as detailed in **??**. The first terms are given by the following,

$$\alpha_c = \underbrace{\alpha_{c,0}}_{1^{\text{st}}\text{ order}} + \underbrace{\alpha_{c,1}\delta}_{2^{\text{nd}}\text{ order}} + \underbrace{\alpha_{c,2}\delta^2}_{3^{\text{rd}}\text{ order}} . \tag{1.3}$$

The expression for δ at first and second order then reads,

$$\begin{aligned} \delta &= -\frac{\Delta f_{RF}}{\alpha_0 f_{RF}} && \Rightarrow \text{Order 1} \\ \delta &= \frac{-\alpha_0 f_{RF} + \sqrt{f_{RF}\left(-4\Delta f_{RF}\alpha_1 + \alpha_0^2 f_{RF}\right)}}{2\alpha_1 f_{RF}} && \Rightarrow \text{Order 2} \end{aligned} \tag{1.4}$$

It is assumed that only the first term is relevant as the induced difference in chromaticity is negligible as will be demonstrated later on. Fig. 1.3 shows the non linearity of the momentum compaction factor and its effect on the calculated δ via the previous formulas.

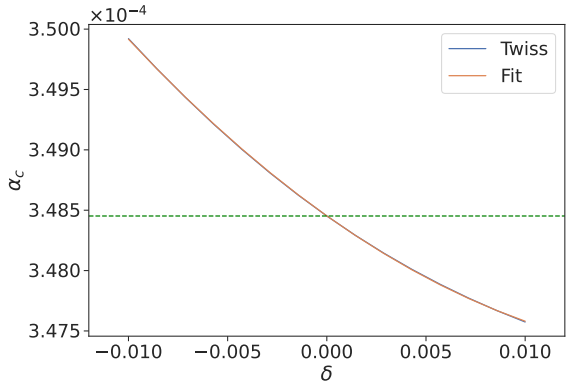

(a) Non-linear fit of α_c obtained via an evaluation at discrete δ in MAD-X. The green line represents a constant $\alpha_c = \alpha_{c,0}$.

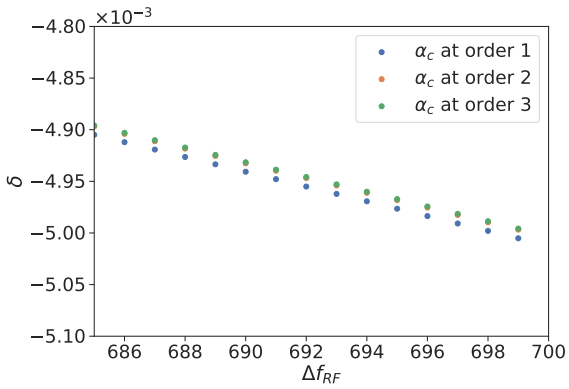

(b) Divergence of the momentum offset when considering higher α_c orders with large RF trims.

Figure 1.3: Non linearity of α_c and its effect on the computed δ via RF trims. The simulations are done at injection energy of 450GeV.

It is observed that while clearly depending on higher orders, the momentum compaction factor only has a small impact on the calculated δ. Fig. 1.4 shows a real-life measurement, comparing the fit of the chromaticity function with various δ, computed up to the third order of α_c.

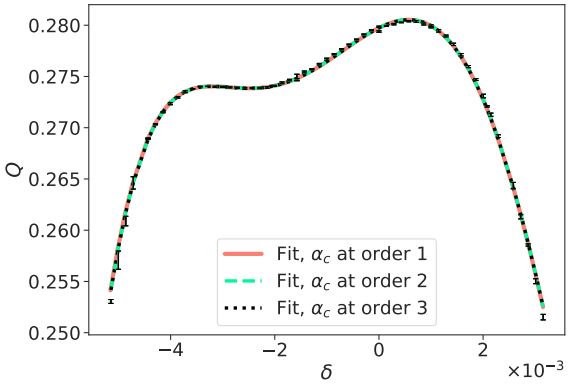

(a) Fit of the chromaticity function at the 5^{th} order, considering the α_c expansion up to the third order.

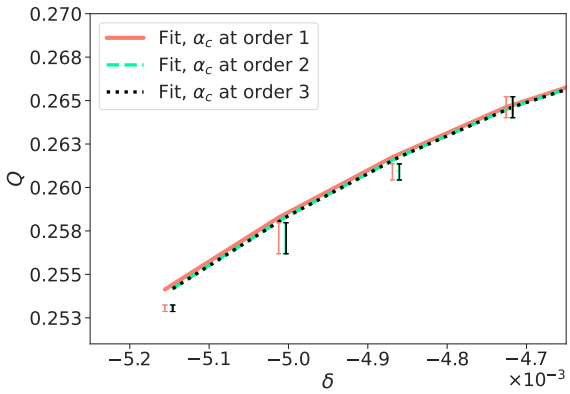

(b) Zoom on one side of the fit. The difference between the second and third order is barely noticeable.

Figure 1.4: Fit of the chromaticity function considering several α_c orders.

The fit of the chromaticity function is barely impacted when considering the higher orders of the momentum compaction factor. The different orders of the chromaticity are collected in Table 1.1. The higher order terms of α_c can thus be neglected and are not a source of higher chromaticity orders.

	α_c order		
Chromaticity	1	2	3
$Q^{(1)}$	2.52 ± 0.03	2.53 ± 0.03	2.53 ± 0.03
$Q^{(2)}$	-3.04 ± 0.05	-3.05 ± 0.05	-3.05 ± 0.05
$Q^{(3)}$	-4.75 ± 0.03	-4.75 ± 0.03	-4.75 ± 0.03
$Q^{(4)}$	-0.33 ± 0.07	-0.32 ± 0.07	-0.32 ± 0.07
$Q^{(5)}$	2.33 ± 0.06	2.36 ± 0.06	2.36 ± 0.06

Table 1.1: Chromaticity values obtained for the same measurement, depending on the order of the momentum compaction factor taken into account.

Momentum Offset from Orbit

During machine operation, the momentum offset, derived from the orbit, used to be logged on the servers. It was then possible to directly compute the chromaticity that way without having to use the RF and the momentum compaction factor. In 2016, measurements of the non-linear chromaticity were performed using the former method. Fig. 1.5 shows a comparison of the obtained non-linear chromaticity from both methods, while Table 1.2 shows a numerical comparison. Results being similar, is it deemed that both methods are reliable to measure the non-linear chromaticity in the LHC.

	δ via RF		δ via orbit	
Plane	$Q''[10^3]$	$Q'''[10^6]$	$Q''[10^3]$	$Q'''[10^6]$
Beam 1				
X	-0.64 ± 0.01	3.00 ± 0.04	-0.62 ± 0.01	2.91 ± 0.04
Y	-0.17 ± 0.01	-2.12 ± 0.04	-0.14 ± 0.01	-2.09 ± 0.04
Beam 2				
X	-1.18 ± 0.02	2.89 ± 0.06	-1.23 ± 0.03	3.13 ± 0.11
Y	0.18 ± 0.02	-1.95 ± 0.05	0.20 ± 0.02	-2.02 ± 0.06

Table 1.2: Comparison of the chromaticity values obtained for the same measurement via two different methods to acquire δ.

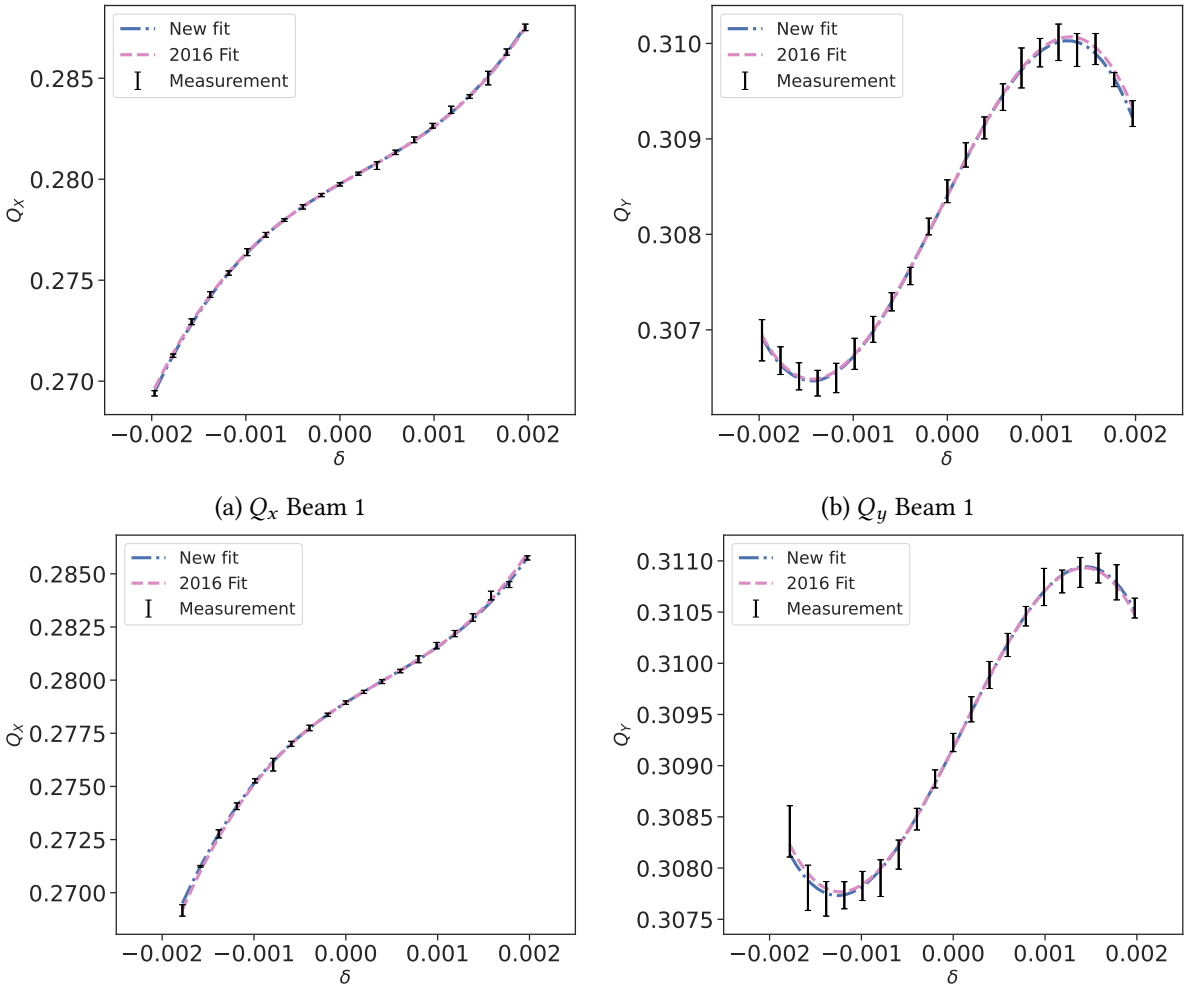

(a) Q_x Beam 1

(b) Q_y Beam 1

(c) Q_x Beam 2

(d) Q_y Beam 2

Figure 1.5: Comparison of the non-linear chromaticity fit obtained from the computed momentum offset via the RF in 2022 and from the logged values in 2016.

1.2.2 Measurements

In order to assess the correctness of the observation of higher chromaticity orders, measurement repeatability is needed. Two measurements were thus take in 2022, with different configurations pertaining to the correction of the second and third order chromaticities Q'' and Q'''. The first one used the nominal correction strengths for octupole and decapole corrector magnets, derived from magnetic measurements, where the second one used beam-based corrections for the same elements, computed from the previous measurement. More measurements were taken during 2024's commissioning

with new optics for the same reasons, to minimize the second and third order chromaticities. Three measurements were taken: with nominal corrections, after having corrected Q''' and then Q''. The introduced new optics mainly changed the powering of the triplets at the IPs and are not expected to have a considerable impact on the chromaticity.

Table 1.3 shows a summary of those measurements with their respective achieved momentum offset ranges. While the 2024 measurements achieved greater ranges than the previous ones, those were restricted during analysis to allow suitable comparisons.

Number	Year	Corrections	δ min. [$\times 10^{-3}$]	δ max. [$\times 10^{-3}$]
1	2022	Nominal	−3.15	3.01
2	2022	Q'' & Q'''	−3.15	3.72
3	2024	Nominal	−5.15	3.15
4	2024	Q'''	−3.44	4.87
5	2024	Q'' & Q'''	−3.86	4.44

Table 1.3: Performed chromaticity measurements with their respective momentum offset ranges.

In order to stay consistent, the horizontal and vertical tunes were respectively set to $Q_x = 0.28$ and $Q_y = 0.31$ for both measurements. The linear chromaticity Q' is set to a small value, around 2, to avoid large tune shifts throughout the scan. All measurements were performed during LHC's beam commissioning, as part of the measurements and corrections performed after technical or long shutdowns.

First Observation

The first observation of higher order chromaticity was done with the octupolar and decapolar correctors *MCO* and *MCD* set to their nominal settings. Those are aimed at correcting Q'' and Q''', as previously described in **??**. Results of this initial measurement are shown in Table 1.4. Lower order chromaticities such as Q' and Q'' are consistent with measurements done during the previous Run [3].

Due to the RF-scan method, the momentum offset crosses zero several times during the measurement. Negligible change in tune at this point makes it possible to determine that the tune drift through the measurement is of no consequence. This measurement was performed after an extended period at injection energy, where the decay of the sextupolar fields is small and not causing any change in the first order chromaticity. The fitted curve for the chromaticity function is shown in Fig. 1.6. It is clear that a higher order polynomial is beneficial to the fit, as discussed further in Section 1.2.2.

Plane	$Q^{(2)}[10^3]$	$Q^{(3)}[10^6]$	$Q^{(4)}[10^9]$	$Q^{(5)}[10^{12}]$
Beam 1				
X	-2.44 ± 0.02	-3.36 ± 0.04	-0.56 ± 0.02	1.20 ± 0.07
Y	0.97 ± 0.02	1.62 ± 0.05	0.15 ± 0.03	-0.88 ± 0.09
Beam 2				
X	-2.45 ± 0.03	-2.72 ± 0.08	-1.00 ± 0.05	0.15 ± 0.14
Y	0.79 ± 0.03	1.54 ± 0.06	0.24 ± 0.04	-0.74 ± 0.13

Table 1.4: Terms of the high order chromaticity obtained during Run 3's commissioning in 2022, with nominal corrections.

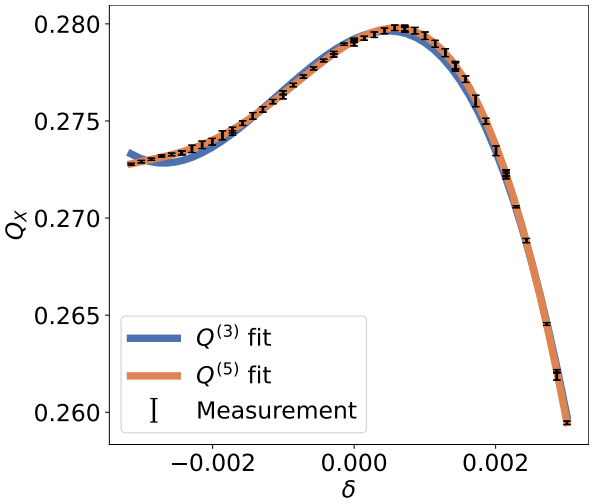

(a) Q_x Beam 1

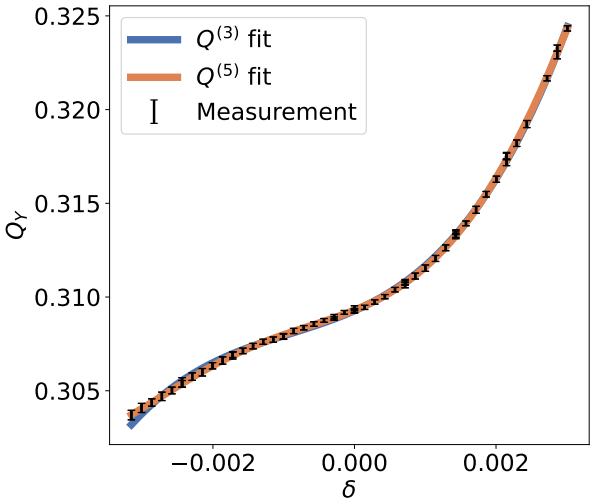

(b) Q_y Beam 1

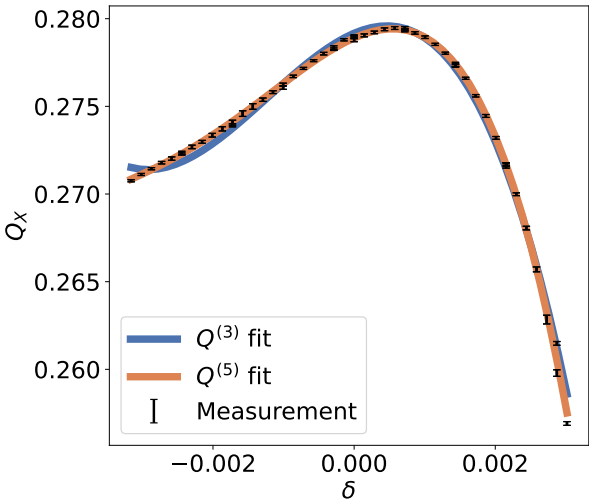

(c) Q_x Beam 2

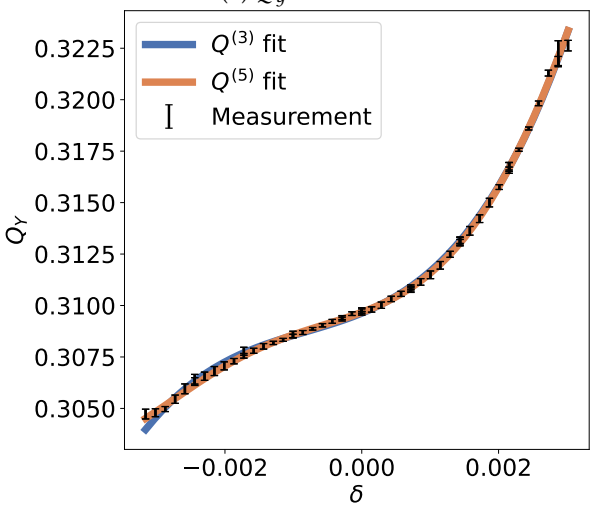

(d) Q_y Beam 2

Figure 1.6: Measurement of higher order chromaticity terms with nominal corrections used during operation. Fits are up to the third and fifth order.

Previous studies of chromaticity in the LHC only considered fits up to the third order. Expanding the fits to the fifth order increases the Q''' estimate and improves the fit quality. Accurately measuring the third order chromaticity is essential for its correction, making it important to consider the higher orders.

Varying Configurations

The five previously introduced measurements were performed with very different configurations for the octupolar and decapolar correctors. Table 1.5 shows the strengths applied on every circuit for each correction scheme, in 2022. The correction is called *global* as all correctors are trimmed uniformly. The 2024 corrections are similar in order of magnitude. Fig. 1.7 shows the measurements and fit of some of these measurements, to highlight their differences.

Beam	$K_4[\mathrm{m}^{-4}]$	$K_5[\mathrm{m}^{-5}]$
1	+3.2973	+1610
2	+2.1716	+1618

Table 1.5: Corrections applied on top of the nominal octupolar and decapolar correctors strengths in 2022 for the Q'' and Q''' corrections.

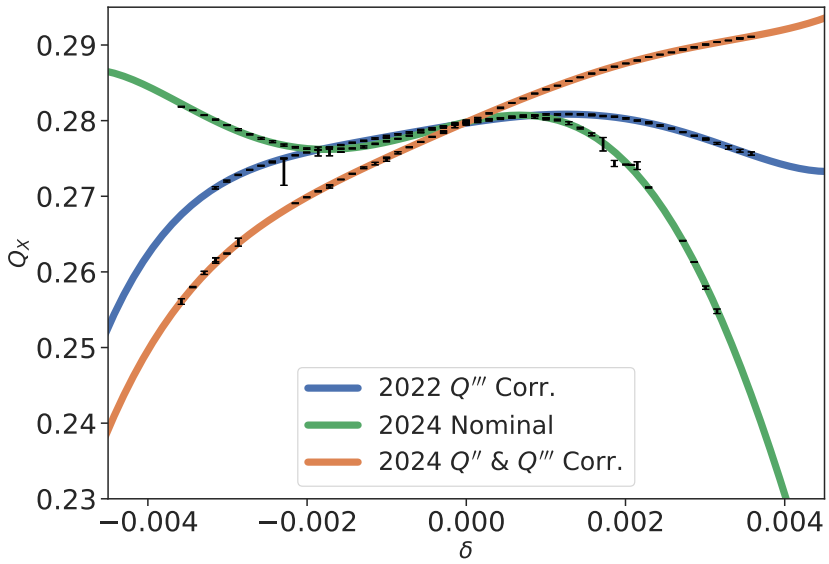

Figure 1.7: Selection of horizontal chromaticity measurements performed with varying configurations of the octupolar and decapolar correctors for Beam 1 during the commissionings of 2022 and 2024.

Axis	Meas.	Q''	Q'''	$Q^{(4)}$	$Q^{(5)}$
Horizontal					
Beam 1	1	-2.44 ± 0.02	-3.37 ± 0.04	-0.56 ± 0.02	1.21 ± 0.07
	2	-0.61 ± 0.01	-1.00 ± 0.03	-0.62 ± 0.02	1.19 ± 0.05
	3	-2.01 ± 0.05	-4.49 ± 0.10	-0.58 ± 0.07	1.34 ± 0.18
	4	-1.46 ± 0.03	-0.29 ± 0.06	-0.43 ± 0.04	1.09 ± 0.10
	5	-0.33 ± 0.01	-0.31 ± 0.03	-0.59 ± 0.01	0.75 ± 0.04
	Avg.			-0.58 ± 0.02	1.00 ± 0.06
Beam 2	2	-0.85 ± 0.01	-0.66 ± 0.03	-0.57 ± 0.02	1.09 ± 0.06
	3	-2.93 ± 0.05	-4.40 ± 0.08	-0.53 ± 0.08	1.66 ± 0.16
	4	-2.21 ± 0.02	-0.00 ± 0.03	-0.46 ± 0.02	1.18 ± 0.05
	5	-0.53 ± 0.02	-0.09 ± 0.03	-0.57 ± 0.02	0.98 ± 0.05
	Avg.			-0.53 ± 0.02	1.10 ± 0.06
Vertical					
Beam 1	1	0.97 ± 0.02	1.62 ± 0.05	0.15 ± 0.03	-0.88 ± 0.09
	2	-0.23 ± 0.01	0.13 ± 0.02	0.09 ± 0.02	-0.60 ± 0.03
	3	0.83 ± 0.02	1.97 ± 0.03	0.29 ± 0.02	-0.68 ± 0.05
	4	0.62 ± 0.01	-0.18 ± 0.03	0.00 ± 0.02	-0.56 ± 0.05
	Avg.			0.13 ± 0.02	-0.62 ± 0.04
Beam 2	1	0.79 ± 0.03	1.54 ± 0.06	0.24 ± 0.04	-0.74 ± 0.13
	2	-0.29 ± 0.01	0.10 ± 0.02	0.13 ± 0.02	-0.58 ± 0.04
	3	0.89 ± 0.02	2.05 ± 0.03	0.32 ± 0.03	-0.73 ± 0.06
	4	0.60 ± 0.02	-0.14 ± 0.03	0.04 ± 0.02	-0.66 ± 0.05
	Avg.			0.14 ± 0.02	-0.64 ± 0.05

Table 1.6: Summary of the chromaticity values obtained from the measurements presented in Table 1.3.

A summary of the measured chromaticity orders is given in Table 1.6. The first measurement in the horizontal plane of Beam 2 showed a high correlation between $Q^{(4)}$ and $Q^{(5)}$, making the fit less reliable and is not included. The last measurement for the vertical plane experienced some tune drift, making the fit impossible and is therefore not included for both beams.

Fit Quality

The values measured for $Q^{(4)}$ and $Q^{(5)}$ are similar across the measurements, with nominal and beam-based corrections performed with very different lower order chromaticity, and well separated in time. This reproducibility with varying configurations gives confidence that the measured values are robust. It is to be noted that one exception exists for the first measurement, the horizontal plane of beam 2 showed a high correlation between the fourth and fifth order terms, making the fit less reliable.

The reduced chi-square for the last measurement of 2022 for each fit order is detailed in Table 1.7. While adding terms to the chromaticity function is beneficial to the fit, it can be seen that the reduced

chi-square does not substantially improve above the fifth order, indicating that such further orders are not warranted.

	χ^2_ν			
Plane	$Q^{(3)}$	$Q^{(4)}$	$Q^{(5)}$	$Q^{(6)}$
Beam 1				
X	17.9	12.1	1.8	1.5
Y	3.0	2.2	0.7	0.7
Beam 2				
X	17.3	7.1	1.8	1.8
Y	2.9	2.8	1.0	1.0

Table 1.7: Reduced χ^2 values for each order of fit, taken from the second measurement of 2022, with Q'' and Q''' beam-based corrections.

1.3 Model Estimates

The model of the LHC is based on MAD-X and WISE field errors [4], containing a hundred seeds for the random errors. To compute the chromaticity, simulations are run via PTC, with various field errors.

1.3.1 Decatetrapolar Decay

It has been noted in the previous chapter about decapoles (see **??**) that the b_5 component in the main dipoles was large at injection energy, and could explain most of the discrepancy between the measurements and simulations. Such a decay in the main dipoles also exists for the b_7 component [5], and is shown in Fig. 1.8.

Its value is though small and settles around $+0.0351 \pm 0.0007$. The average b_7 of the main dipoles is of 0.32 ± 0.16. The decay thus increase that value of only about 11%. Simulations done with that decay taken into account are detailed next.

1.3.2 Major contributions

Simulations with various field errors have been run to assess the contribution of individual magnet order and combinations for the fourth and firth order chromaticity. Normal and skew fields errors ranging from sextupolar (b_3) to decahexapolar (b_8) are added alone or in combination to observe which is the strongest. Quadrupolar field errors (b_2) introduce beta-beating. Coupling is introduced via skew quadrupolar correctors.

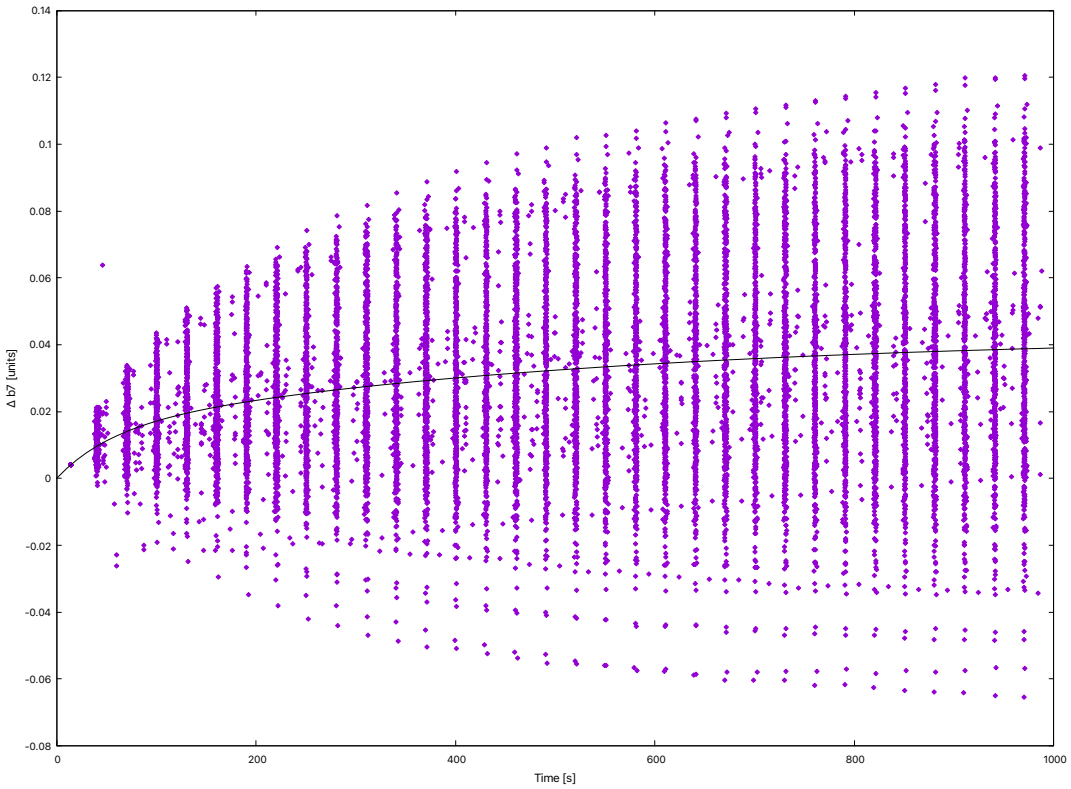

Figure 1.8: Measured decay of the integrated decatetrapolar field in LHC's main dipoles at injection energy. The fit is shown in black [5] and settles around +0.035.

Fourth Order Chromaticity

The results from simulations strongly imply that the dodecapolar errors are the main contributors to $Q^{(4)}$, as can be seen in Fig. 1.9. Fringe fields have a negligible impact, as do skew multipoles. The most notable effect on this chromaticity order is the beta-beating, introducing a very large spread via the various error seeds. Comparing the simulation at the top with most errors added, the b_6 component alone accounts for $\approx 70\%$ of it for both axes on each beam.

Fifth Order Chromaticity

It is seen that the the decatetrapolar errors are the main contributors to $Q^{(5)}$, as can be seen in Fig. 1.10. Fringe fields and skew multipoles have been found to have a negligible impact. Beta-beating and coupling are seen to increase by a small amount the chromaticity, while sextupolar errors induce a spread with the different seeds. As for the fourth order, comparing the simulation at the top with most errors added, the b_7 component alone accounts for $\approx 70\%$ of it for both axes on each beam of the fifth

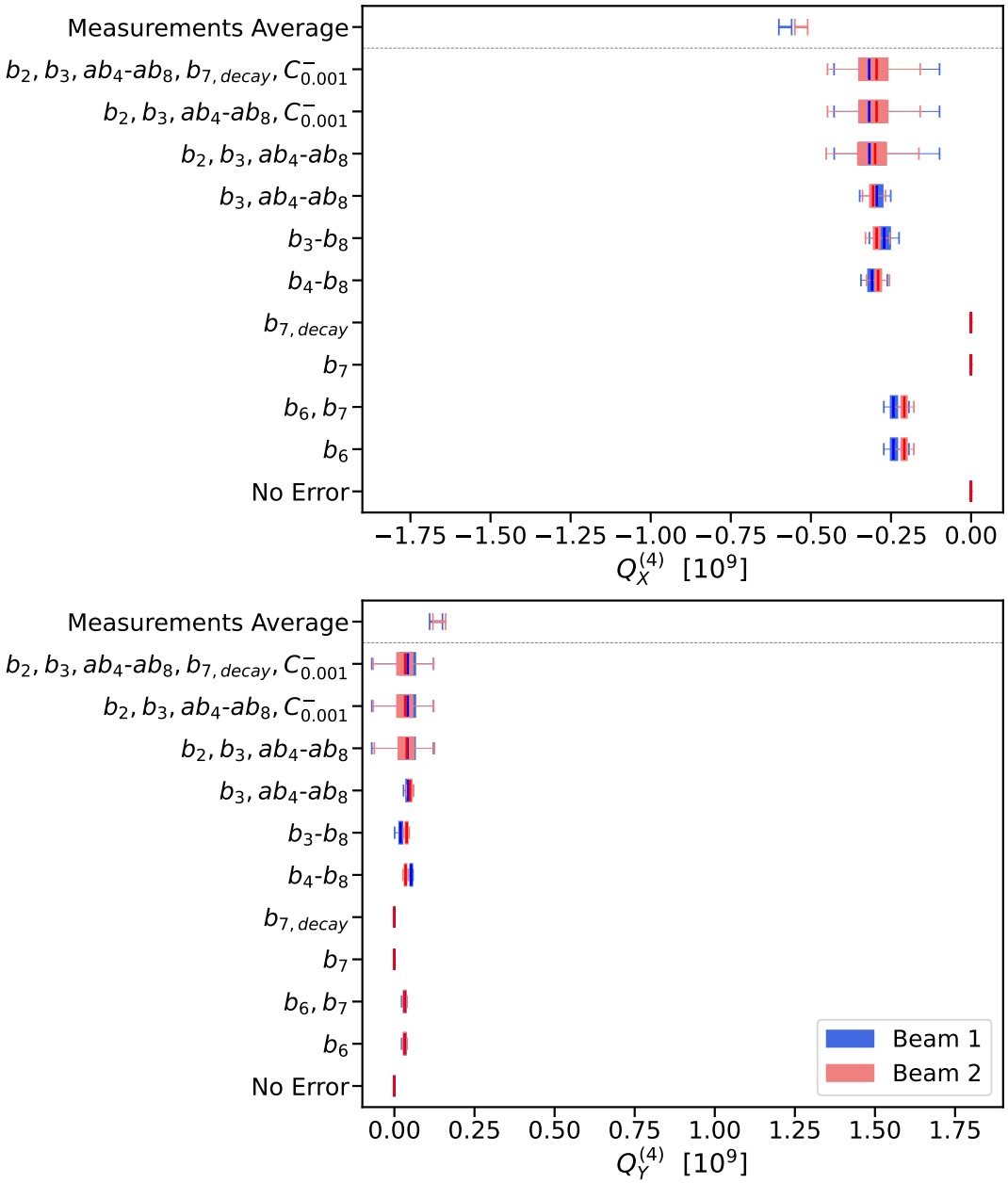

Figure 1.9: Measured and simulated fourth order chromaticity with different multipole errors. The b_2 errors, applied on dipoles and quadrupoles, generate beta-beating. Coupling is set to a value commonly seen in operation.

order chromaticity.

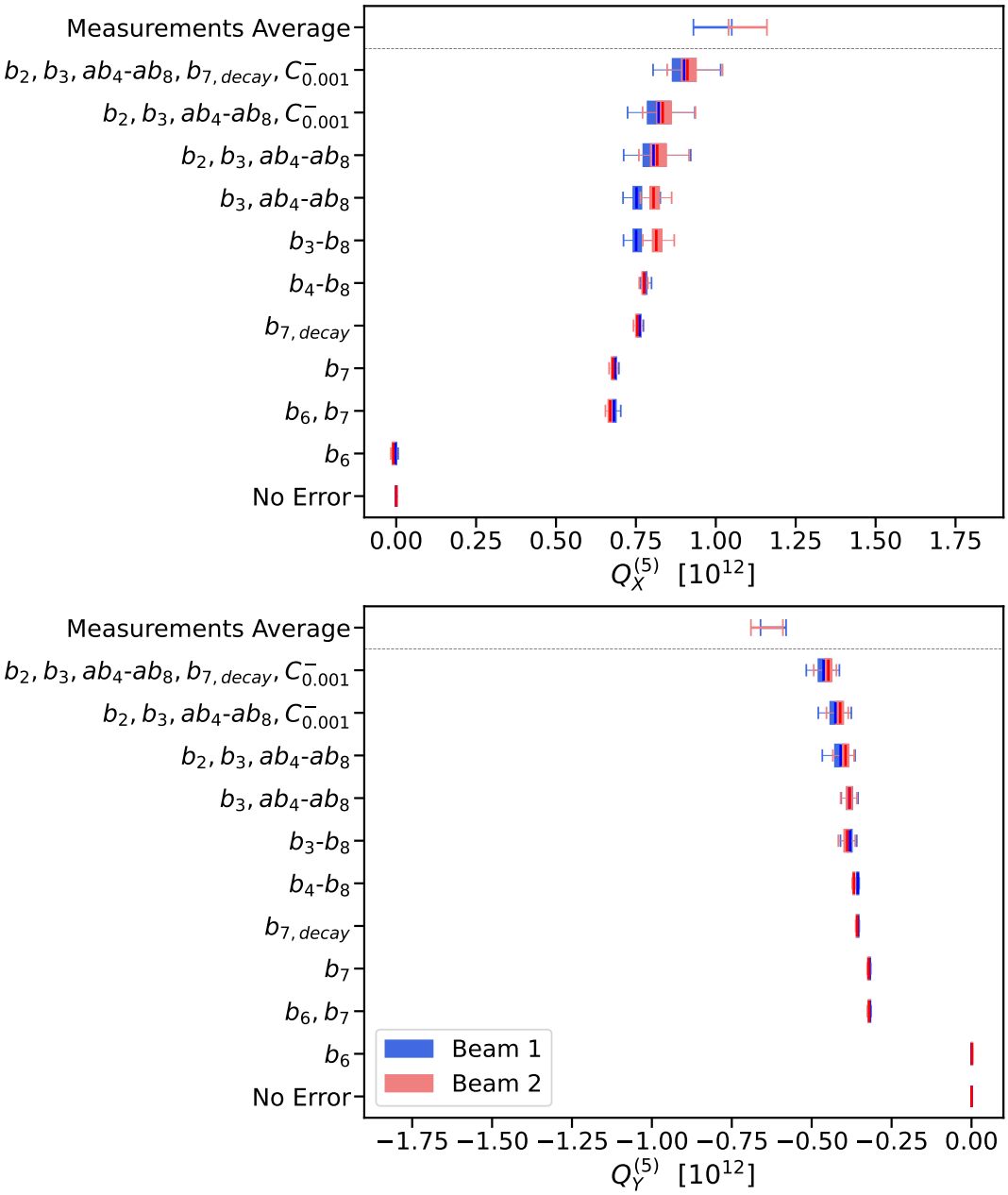

Figure 1.10: Measured and simulated fifth order chromaticity with different multipole errors. The b_2 errors, applied on dipoles and quadrupoles, generate beta-beating. Coupling is set to a value commonly seen in operation.

1.3.3 Ratios

Previous simulation results are shown in Table 1.8, taking the values from the simulation including the most effects at the top of the plots. For the fourth order, the beating is not included as the large beating is not yet explained. Table 1.9 shows the ratio between the measured average and simulated chromaticities.

Plane	$Q^{(4)}\,[10^9]$	$Q^{(5)}\,[10^{12}]$
Beam 1		
X	-0.29 ± 0.02	0.90 ± 0.05
Y	0.04 ± 0.01	-0.46 ± 0.03
Beam 2		
X	-0.31 ± 0.02	0.92 ± 0.03
Y	0.05 ± 0.00	-0.45 ± 0.01

Table 1.8: Simulated high order chromaticity terms via PTC at injection energy, including normal and skew sextupolar to decahexapolar field errors. Are also included beta-beating, coupling and decatetrapolar decay. For the fourth order, the values do not include beta-beating as the observed spread is not yet fully understood.

Plane	$Q^{(4)}$ Ratio	$Q^{(5)}$ Ratio
Beam 1		
X	1.98 ± 0.16	1.10 ± 0.09
Y	3.00 ± 0.70	1.34 ± 0.11
Beam 2		
X	1.74 ± 0.11	1.20 ± 0.08
Y	2.90 ± 0.50	1.42 ± 0.12

Table 1.9: Ratios of the simulated and average measured high-order chromaticity terms. The values are taken from Table 1.6 and Table 1.8.

The similar ratios between planes and beams for the fifth order could indicate a systematic error not modeled. The plane differences for the fourth order are not yet explained but could be linked to a lack of clear reproducibility induced by lower orders in the vertical plane. It indeed seems that the fourth order follows a trend with the third order.

1.4 Dodecapolar RDTs

b6 meas from 2024 commissioning

1.5 Going Further

2024 chromaticity measurements without range cutting.

1.6 Summary

A wider momentum offset range, combined with new analysis techniques permitted the observation of the fourth and fifth order of the chromaticity function for the first time in the LHC. Reproducible values were measured with different machine configurations.

Simulations show that the observed values do not match well with the LHC non-linear model. A factor ≈ 1.5 is observed between measurements and simulations for $Q^{(5)}$, which may point to a systematic error in the b7 error model.

Correction of the measured higher order chromaticity terms is not possible, due to the lack of adequate correctors in the LHC. It is nevertheless interesting to characterize the higher order errors for an effective model and understand the effect a higher order fit has on lower order terms. Precise measurement of those lower chromaticity terms is required in order to effectively correct them. Higher order terms have thus to be taken into account.

The current range of momentum offset is deemed sufficient to measure higher order chromaticity. Attempts will, however, be taken to increase that range and assess if such a wider range can refine the estimate of $Q^{(4)}$ and $Q^{(5)}$.